

Lysozyme purification with dye-affinity beads under magnetic field

Nilgün Başar, Lokman Uzun, Ali Güner, Adil Denizli*

Department of Chemistry, Hacettepe University, Ankara, Turkey

Received 14 December 2006; received in revised form 23 February 2007; accepted 23 February 2007

Available online 2 March 2007

Abstract

Magnetic poly(2-hydroxyethyl methacrylate) mPHEMA beads carrying Cibacron Blue F3GA were prepared by suspension polymerization of HEMA in the presence of Fe_3O_4 nano-powder. Average size of spherical beads was 80–120 μm . The beads had a specific surface area of 56.0 m^2/g . The characteristic functional groups of dye-attached mPHEMA beads were analyzed by Fourier transform infrared spectrometer (FTIR) and Raman spectrometer. mPHEMA with a swelling ratio of 68% and carrying 28.5 μmol Cibacron Blue F3GA/g were used for the purification of lysozyme. Adsorption studies were performed under different conditions in a magnetically stabilized fluidized bed (i.e., pH, protein concentration, flow-rate, temperature, and ionic strength). Lysozyme adsorption capacity of mPHEMA and mPHEMA/Cibacron Blue F3GA beads were 0.8 mg/g and 342 mg/g, respectively. It was observed that after 20 adsorption–desorption cycle, mPHEMA beads can be used without significant loss in lysozyme adsorption capacity. Purification of lysozyme from egg white was also investigated. Purification of lysozyme was monitored by determining the lysozyme activity using *Micrococcus lysodeikticus* as substrate. The purity of the desorbed lysozyme was about 87.4% with recovery about 79.6%. The specific activity of the desorbed lysozyme was high as 41.586 U/mg.
© 2007 Elsevier B.V. All rights reserved.

Keywords: Affinity chromatography; Lysozyme; Protein purification; Magnetic beads; Magnetic field

1. Introduction

The development of techniques and methods for the separation and purification of proteins has been essential for many of the recent advancements in biotechnology and biomedical research [1]. The purity of a protein is a pre-requisite for its structure and function studies or its potential application [2]. A wide variety of protein purification techniques are available today, however, different types of chromatography have become dominant due to their high resolving power [3]. In gel filtration chromatography, dye-affinity chromatography, ion-exchange chromatography, immobilized metal-ion affinity chromatography, bioaffinity chromatography and hydrophobic interaction chromatography (HIC), the protein separation is dependent on their biological and physico-chemical properties; molecular size, net charge, biospecific characteristics and hydrophobicity, respectively [4–6].

Dye–ligand chromatography has been used extensively in laboratory and large-scale protein purification [7–9]. Dye–ligands are commercially available, inexpensive, and can easily be immobilized, especially on matrices bearing hydroxyl groups. Although dyes are all synthetic in nature, they are still classified as affinity ligands because they interact with the active sites of many proteins mimicking the structure of the substrates, cofactors, or binding agents for those proteins. A number of textile dyes, known as reactive dyes, have been used for protein purification. Most of these reactive dyes consist of a chromophore (either azo dyes, anthraquinone, or phthalocyanine), linked to a reactive group (often a mono- or dichloro-triazine ring). The interaction between the dye ligand and proteins can be by complex combination of electrostatic, hydrophobic, hydrogen bonding. Cibacron Blue F3GA is an anthraquinone textile dye that interacts specifically and reversibly with albumin [10].

Lysozyme (*N*-acetylmuramide glyconohydrolase) is one of the best characterized hydrolases. Lysozyme is considered to be a self-defense enzyme, which is produced in serum, mucus and many organs of vertebrates. Lysozyme is found in a variety of vertebrate cells and secretions, such as spleen, milk, tears and egg white. Lysozyme lyses certain bacteria by hydrolyzing the β -linkages between the muramic acid and *N*-acetylglucosamine of

* Corresponding author at: P.K. 1, Samanpazarı, 06242 Ankara, Turkey.
Tel.: +90 312 2992163; fax: +90 312 2992163.

E-mail address: denizli@hacettepe.edu.tr (A. Denizli).

the mucopolysaccharides which are present in the bacterial cell wall. Lysozyme is a commercially valuable enzyme, which has tremendous potential for application in pharmaceutical and food industries. Its common applications are as a cell disrupting agent for extraction of bacterial intracellular products, as an antibacterial agent in ophthalmologic preparations, as a food additive in milk products and as a drug for treatment of ulcers and infections [11]. The potential for its use as an anticancer drug has been demonstrated by animal and in vitro cell culture experiments [12]. Lysozyme has also been used in cancer chemotherapy [13]. In a recent article, it has been reported that lysozyme can be used for increasing the production of immunoglobulin by hybridoma technology [14]. The large-scale applications require more efficient and cost effective techniques for its isolation [15].

Magnetic separation techniques have currently found many applications in different area of biosciences, especially in laboratory scale [16]. Magnetic separation promises to solve many of the problems associated with chromatographic techniques in packed bed and in conventional fluidized bed systems [17]. The magnetic character implies that they respond to a magnet, making sampling and collection easier and faster, but their magnetization disappears once the magnetic field is removed. Magnetic carriers combine some of the best characteristics of fluidized beds (low pressure drop and high feed-stream solid tolerances) and of fixed beds (high mass transfer rates, and good fluid–solid contact). Magnetic separation is requiring a simple apparatus, composed to centrifugal separation. Recently, there has been increased interest in the use of magnetic carriers in biomolecule coupling, nucleic acid and protein purification [18–22].

The aim of our study is to prepare a dye-affinity magnetic adsorbent, for efficient separation of lysozyme from aqueous solutions and chicken egg white in a magnetically stabilized fluidized bed (MSFB) system. The efficient mass transfer properties of MSFBs makes them appropriate candidates as the basis for such chromatographic processes. Lysozyme adsorption properties of the mPHEMA beads from aqueous solutions were investigated at different experimental conditions. Desorption of lysozyme and reusability of the adsorbents were also tested. Finally, the dye-affinity beads were used for the purification of lysozyme from egg white. The purity of the desorbed lysozyme was determined by SDS-PAGE and the activity of the desorbed lysozyme was measured using *Micrococcus lysodeikticus* as a substrate microorganism.

2. Experimental

2.1. Materials

Lysozyme (chicken egg white, EC 3.2.1.7) and Cibacron Blue F3GA were supplied by Sigma (St. Louis, MO, USA) and used as received. The monomers used, 2-hydroxyethyl methacrylate (HEMA) and ethylene glycol dimethacrylate (EGDMA) were purchased from Sigma and inhibitor was removed using a column of basic alumina prior to use. Magnetite nanopowder (Fe₃O₄, average diameter: 20–50 nm) was obtained from Sigma. Benzoyl peroxide was obtained from Fluka (Switzer-

land). Azobisisobutyronitrile (AIBN, Sigma) was selected as the initiator. AIBN was recrystallized from methanol. Poly(vinyl alcohol) (98% hydrolyzed) was obtained from Aldrich Chemical Co. (USA) and had a molecular weight of 100,000 by viscosity. All other chemicals were guaranteed or analytical grade reagents commercially available and used without further purification. Laboratory glassware was kept overnight in a 5% nitric acid solution. Before use the glassware was rinsed with deionised water and dried in a dust-free environment. All water used in the adsorption experiments was purified using a Barnstead (Dubuque, IA, USA) ROpure LP[®] reverse osmosis unit with a high-flow cellulose acetate membrane (Barnstead D2731) followed by a Barnstead D3804 NANOpure[®] organic/colloid removal and ion-exchange packed-bed system.

2.2. Preparation of mPHEMA particles

mPHEMA particles were produced by suspension polymerization in an aqueous medium as described in our previous articles [23]. Polymerization procedure of mPHEMA particles was given as below: the dispersion medium was prepared by dissolving 200 mg of poly(vinyl alcohol) within 50 ml of distilled water. The desired amount of 2,2'-azobisisobutyronitrile (0.06 g) was dissolved within the monomer phase 12/4/8 ml (EGDMA/HEMA/toluene) with 1.0 g of magnetite particles. This solution was then transferred into the dispersion medium placed in a magnetically stirred (at a constant stirring rate of 600 rpm) glass polymerization reactor (100 ml) which was in a thermostatic water bath. The reactor was flushed by bubbling nitrogen and then was sealed. The polymerization was allowed to proceed under nitrogen atmosphere at 65 °C for 4 h and finally at 90 °C for 2 h. This reaction led to the formation of white beads. After polymerization, mPHEMA particles were separated from the polymerization medium. Then, the beads were placed in a Soxhlet extraction apparatus, and the porogenic solvents were extracted out of the beads with acetone under reflux for at least 12 h. The beads were dried undervacuum at room temperature. The dried beads were fractionated by sieving with standard test sieves.

2.3. Cibacron Blue F3GA-attached mPHEMA beads

Ten grams of mPHEMA beads was magnetically stirred (at 400 rpm) in a sealed reactor at a constant temperature of 80 °C for 4 h with 100 ml of the Cibacron Blue F3GA aqueous solution containing 4.0 g NaOH. The initial concentration of the Cibacron Blue F3GA in the medium was 1.0 mg/ml. After incubation, the Cibacron Blue F3GA-attached beads were filtered, and washed with distilled water and methanol several times until all the physically adsorbed Cibacron Blue F3GA molecules were removed. The modified beads were stored at 4 °C with 0.02% sodium azide to prevent microbial contamination. The leakage of the Cibacron Blue F3GA from the beads was followed by treating the magnetic beads with fresh human plasma samples for 24 h at room temperature. Cibacron Blue F3GA released after this treatment was measured in the liquid phase by spectrophotometry at 630 nm.

The characteristic functional groups of dye and polymeric beads were analyzed by using a Fourier transform infrared spectrophotometer (FTIR, 8000 Series, Shimadzu, Japan). The samples were prepared by mixing with approximately 100 mg of dry, powdered KBr (0.1 g, IR Grade, Merck, Germany), and pressed into a pellet form. The FTIR spectrum was then recorded.

Raman spectra of polymeric samples were recorded using Labram HR Raman spectrometer (Jobin Yvon) with a He–Ne Laser source emitting at 633 nm, 600–1200 grooves/mm holographic grating and a charge coupled device (CCD) detector. Raman spectra were obtained in 250 s integrations with an average three scans. Spectra were recorded with reproducibility within 1 cm^{-1} , hole $400\text{ }\mu\text{m}$, slit $150\text{ }\mu\text{m}$ and resolution $0.1\text{ }\mu\text{m}$.

2.4. Lysozyme adsorption–desorption studies from aqueous solutions

Chromatographic adsorption studies were carried out on a magnetically stabilized fluidized bed system by using BioRad economic column (diameter: 1 cm, length: 10 cm). Magnetic beads suspended in pure water were put into a column equipped with a water jacket for temperature control. Expanding of the mag-beads was done conventionally. During the experiment, the magnetic beads in the column were exposed to magnetic field which surrounded the column ($B_{\text{rms}} \approx 24\text{ G}$, $B_{\text{p-p}} \approx 33\text{ G}$, $\phi = 50\text{ Hz}$). In a typical adsorption system, 100 ml of the lysozyme solution was passed through the column containing magnetic beads, by a peristaltic pump for 2 h. Dynamic binding capacity (DBC) was calculated from lysozyme breakthrough curves. Equilibration of Cibacron Blue F3GA-attached mPHEMA column was performed by passing four column volumes of sodium acetate buffer (pH 5.2) before injection of the lysozyme solution. Effects of the lysozyme concentration, pH of the medium, flow-rate, temperature and ionic strength on the adsorption capacity were studied. To observe the effects of the initial concentration of lysozyme on adsorption, it was changed between 0.5 mg/ml and 3.0 mg/ml. To determine the effect of pH on the adsorption, pH of the solution was changed between 5.0 and 9.0. The flow-rate of the lysozyme solution was varied between 0.5 ml/min and 3.5 ml/min. To observe the effects of ionic strength, firstly; the adsorption experiments were carried out in salt free solutions and then, they were repeated in solutions containing NaCl. The concentration of NaCl were changed between 0.01 M and 0.1 M. Lysozyme concentration was determined by Bradford method at 595 nm. The adsorption experiments were performed in replicates of three and the samples were analyzed in replicates of three as well. For each set of data present, standard statistical methods were used to determine the mean values and standard deviations. Confidence intervals of 95% were calculated for each set of samples in order to determine the margin of error.

2.5. Desorption and repeated use

Desorption of lysozyme was studied with 0.1 M Tris/HCl buffer containing 0.5 M NaCl. In a typical desorption experi-

ment, 50 ml of the desorption agent was pumped through the column at a flow-rate of 1.0 ml/min for 1 h. When desorption was achieved, the column was cleaned with 50 mM NaOH and then re-equilibrated with 25 mM sodium acetate buffer containing 0.1 M NaCl (pH 7.4). The final lysozyme concentration in elution medium was determined spectro-photometrically. Desorption ratio was calculated from the amount of lysozyme adsorbed on the mPHEMA beads and the final lysozyme concentration in elution medium.

In order to test the reusability of the dye-attached mPHEMA beads, lysozyme adsorption–elution procedure was repeated 20 times by using the same magnetic column. In order to regenerate and sterilize, after elution; the beads were washed with 50 mM NaOH solution.

To evaluate the effects of the adsorption conditions on the lysozyme structure, the fluorescence spectra of the native lysozyme, heat-denatured lysozyme (at $72\text{ }^\circ\text{C}$), and desorbed lysozyme were recorded. Native lysozyme (1.0 mg/ml, pH 7.0) was incubated at $70\text{ }^\circ\text{C}$ for 8 h for denaturation. Fluorimetric measurements were taken with a Shimadzu spectrofluorometer (Tokyo, Japan) with 1 cm quartz cells. Monochromatic readings were taken from a digital display with a 0.25 s time constant and with a 3 nm band width on the excitation side and a 5 nm band width on the emission side. The initial calibration was carried out with a standard solution of lysozyme in phosphate-buffered saline with a 280-nm fluorescence excitation wavelength and a 340 nm emission wavelength.

2.6. Purification of lysozyme from egg white

Chromatographic purification was carried out on a magnetically stabilized fluidized bed system by using BioRad economic column (diameter: 1 cm, length: 10 cm). Magnetic beads suspended in pure water were put into a column equipped with a water jacket for temperature control. Expanding of the magnetic beads was done conventionally. During the experiment, the magnetic beads in the column were exposed to magnetic field which surrounded the column ($B_{\text{rms}} \approx 24\text{ G}$, $B_{\text{p-p}} \approx 33\text{ G}$, $\phi = 50\text{ Hz}$). Chicken egg white was separated from fresh eggs and diluted to 50% (v/v) with phosphate buffer (100 mM, pH 7.0). The diluted egg white was homogenised in an ice bath and centrifuged at $4\text{ }^\circ\text{C}$, at 10,000 rpm for 30 min. Then, diluted egg white solution was pumped through the column at a flow-rate of 1.0 ml/min for 2 h. Later, the desorption of lysozyme from the magnetic beads was performed with 0.1 M Tris–HCl buffer containing 0.5 M NaCl under magnetic field. The activity of desorbed lysozyme was determined spectrophotometrically at 620 nm, the decrease in the turbidity of culture of *M. lysodeikticus* cells suspended in phosphate buffer (0.1 M, pH 7.0) was followed for 5 min after addition of lysozyme. One unit of lysozyme activity was defined as the amount of enzyme causing a decrease of 0.001 optical density value per minute at $25\text{ }^\circ\text{C}$ and pH 7.0.

The purity of lysozyme in the purified samples was assayed by sodium dodecylsulfate-polyacrylamide gel electrophoresis (SDS-PAGE) using 10% separating gel $9\text{ cm} \times 7.5\text{ cm}$ and 6% stacking gels were stained with 0.25% (w/v) Coomassie Brilliant R 250 in acetic acid–methanol–water (1:5:5, v/v/v) and

destained in ethanol–acetic acid–water (1:4:6, v/v/v). Electrophoresis was run for 2 h with a voltage of 110 V. Human serum albumin and IgG were used as standards.

3. Results and discussion

3.1. Properties of magnetic particles

Magnetically stabilized fluidized bed was used as an affinity adsorption column for lysozyme purification. Cibacron Blue F3GA was used as the dye–ligand for specific binding of protein molecules. mPHEMA particles were selected as the carrier matrix and produced by suspension technique. Cross-linked PHEMA hydrogels are hydrophilic polymer networks capable of imbibing large amounts of water yet remain insoluble and preserve their three-dimensional shape. Some properties of the mPHEMA particles were summarized in Table 1. The simple incorporation of water weakens the secondary bonds within the hydrogels. This enlarges the distance between the polymer chains and causes swelling.

The surface morphology and internal structure of non-magnetic PHEMA and mPHEMA beads are exemplified by the scanning electron pictures in Fig. 1. As seen in Fig. 1A, mPHEMA beads have a spherical form and a rough surface containing macropores due to the abrasion of magnetite crystals (diameter <20–50 nm) during the polymerization procedure. However, the surface of the non-magnetic spherical PHEMA beads contained no macropores (Fig. 1B). The pictures in Fig. 1C and D were taken with broken beads to observe the internal parts

Table 1
Some properties of the mPHEMA particles

Particle diameter	80–120 μm
Specific surface area	56 m^2/g
Average pore size	819 nm
Swelling ratio	45%
Cibacron Blue F3GA content	28.5 $\mu\text{mol}/\text{g}$
Density	1.1 g/ml
Volume fraction of polymer	94.5%
Volume fraction of magnetite particles	5.5% Fe_3O_4
Magnetic field resonance	2250 G

of both non-magnetic and magnetic PHEMA beads. The presence of macropores within the bead interior was clearly seen in these photographs. It can be concluded that the mPHEMA beads have a macroporous interior surrounded by a reasonably rough surface, in the dry state. On the other hand, non-magnetic PHEMA beads were in the uniform and spherical shape with smooth surface characteristics.

3.2. Spectroscopic characterization of beads

Evaluation of the IR spectrum (Fig. 2B) of cross-linked mPHEMA beads shows that the broad peak of O–H stretching vibration of HEMA monomer at 3452 cm^{-1} has disappeared. Multiple sharp peaks at 3500 cm^{-1} frequency range characterized especially the OH stretching vibration that is added and not added to the hydrogen bonding. However, the point which should be stressed is that; electrostatic interaction also occurs between the Fe^{3+} ion and OH group besides the hydrogen bonds

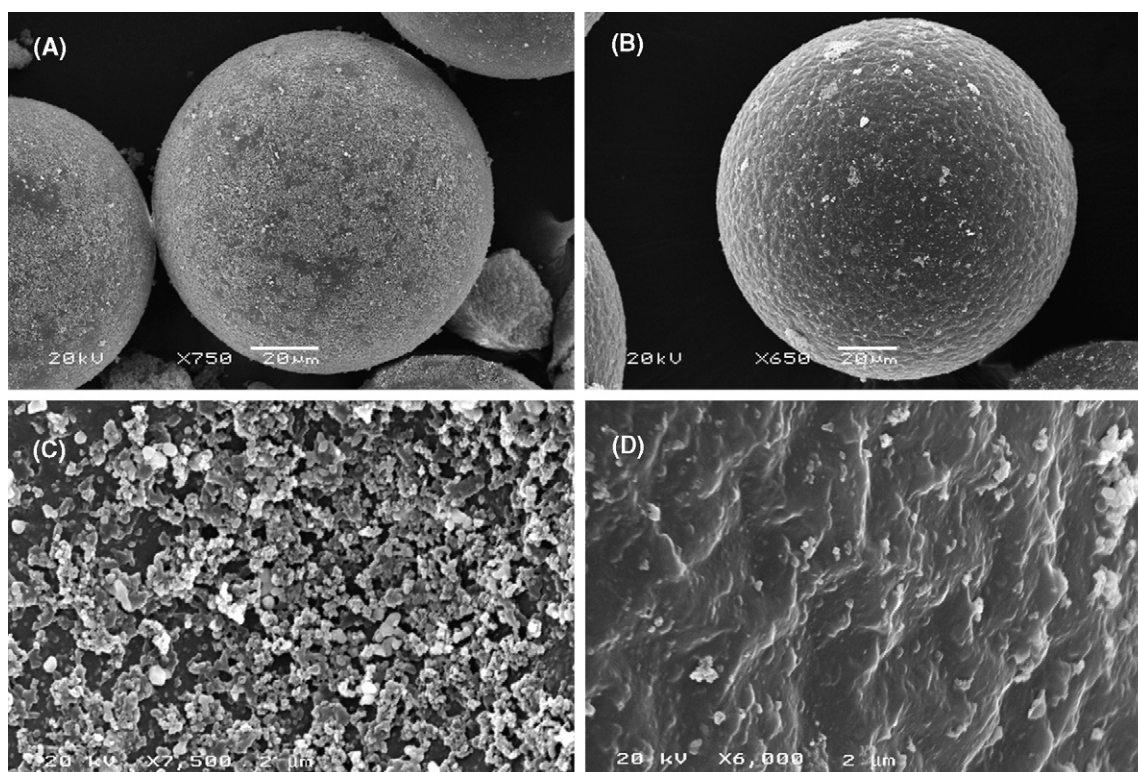


Fig. 1. SEM pictures of polymeric beads: (A) mPHEMA beads; (B) non-magnetic PHEMA beads; (C) cross-section of mPHEMA beads; (D) cross-section of non-magnetic PHEMA beads.

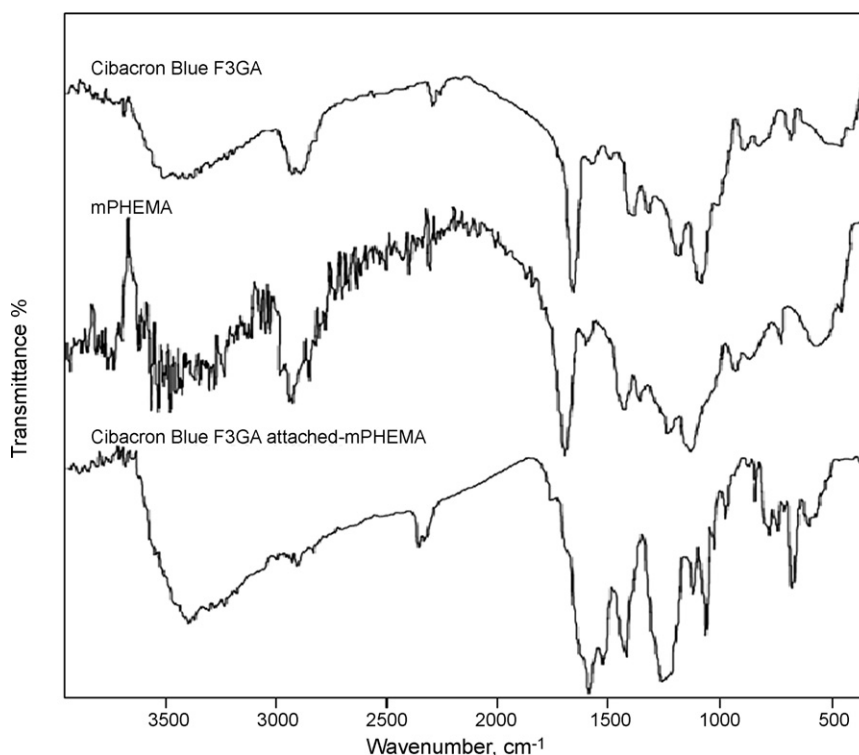


Fig. 2. FTIR spectra of: (A) mPHEMA beads; (B) Cibacron Blue F3GA; (C) Cibacron Blue F3GA-attached mPHEMA beads.

between the OH group itself. That is why the broad peak of OH in the spectrum of HEMA is not manifested in the spectrum taken in the presence of Fe^{3+} .

FTIR spectrum of Cibacron Blue F3GA is given in Fig. 2A. The N–H stretching vibration bands of this dye appear at 3455 cm^{-1} frequency range as multiple bands. The different amine groups of the dye could have a tendency to be free and H-bonded. That is why this spectral situation is regular. The band having moderate intensity at 1739 cm^{-1} , a shoulder at 1650 cm^{-1} and then sharp bands at 1565 cm^{-1} and 1507 cm^{-1} are the spectral evidences that characterize the C=O, C=N and C=C stretching vibrations of the structure. The band at 1226 cm^{-1} and the broad band at nearly 25 cm^{-1} below and above this frequency characterize the S=O stretching vibrations. The band that can be seen obviously at 1085 cm^{-1} belongs to the C–Cl stretching. At the lower wavenumber such as 1022 cm^{-1} S–O stretching vibration band is also seen in the spectrum. In addition, it is possible to see the C–Cl stretching vibrations of the dye at different wavenumbers in the range of $500\text{--}700\text{ cm}^{-1}$.

Fig. 2C shows the IR spectrum of Cibacron Blue F3GA-attached mPHEMA beads. The C=O band is observed at 1727 cm^{-1} as a sharp peak. It implies that the strength of the band at 1650 cm^{-1} is very low. The peaks at 1262 cm^{-1} and 1158 cm^{-1} characterize the C–O stretching vibrations. The conversion of the C–Cl stretching vibration of the original Cibacron Blue F3GA at 1085 cm^{-1} to a weak shoulder at 1081 cm^{-1} of the IR bands. In addition the decrease in the intensity of the same stretching vibrations of Cibacron Blue F3GA at $500\text{--}700\text{ cm}^{-1}$ frequency interval.

Fig. 3A shows the Raman spectrum of mPHEMA beads. According to the evaluation of the Raman spectrum of the polymer, Raman band of the C=O stretching vibration appears at 1724.5 cm^{-1} . If we remember that the same stretching vibration took place at 1724 cm^{-1} in IR spectrum. It can be said that a spectral evaluation integrity is provided. It allows one to notice that the C=O stretching vibration bands are seen over 1724.5 cm^{-1} as a shoulder when it is taken into account that the different carbonyl groups take place in the composite structure. The peak of the terminal --C=CH_2 group of the EGDMA at 1637 cm^{-1} in IR spectrum, occurs at 1638.2 cm^{-1} frequency value in Raman spectrum. There is a spectral evidence that the strong Raman band at 1317 cm^{-1} characterizes the C–O stretching vibration. The stretching vibrations of the Fe–O are obtained over 800 cm^{-1} , 400 cm^{-1} and nearly 200 cm^{-1} as characteristic Raman bands [24]. When the Raman spectrum of the sample is evaluated, we can clearly see three Raman bands characterizing, respectively, the Fe–O stretching vibrations at 815 cm^{-1} , 412 cm^{-1} and 229 cm^{-1} .

When the Raman spectrum of this system is considered, at the neighbouring wavenumber the C=O, C=N and C=C stretching vibrations that support the evidence of the IR spectrum (Fig. 3B) appeared as strong Raman bands at 1795 cm^{-1} , 1638 cm^{-1} and 1593 cm^{-1} , respectively. The two Raman bands 1252 cm^{-1} and 1161 cm^{-1} characterize the S=O stretching vibration of the dye. The stretching vibration band of the C–Cl at 1085 cm^{-1} in the Raman spectrum displayed as a weak Raman band. However, two bands that characterize this stretching vibration occur at 716 cm^{-1} and 659 cm^{-1} , respectively. When the Raman spectrum is evaluated, in plane and out of plane bendings and

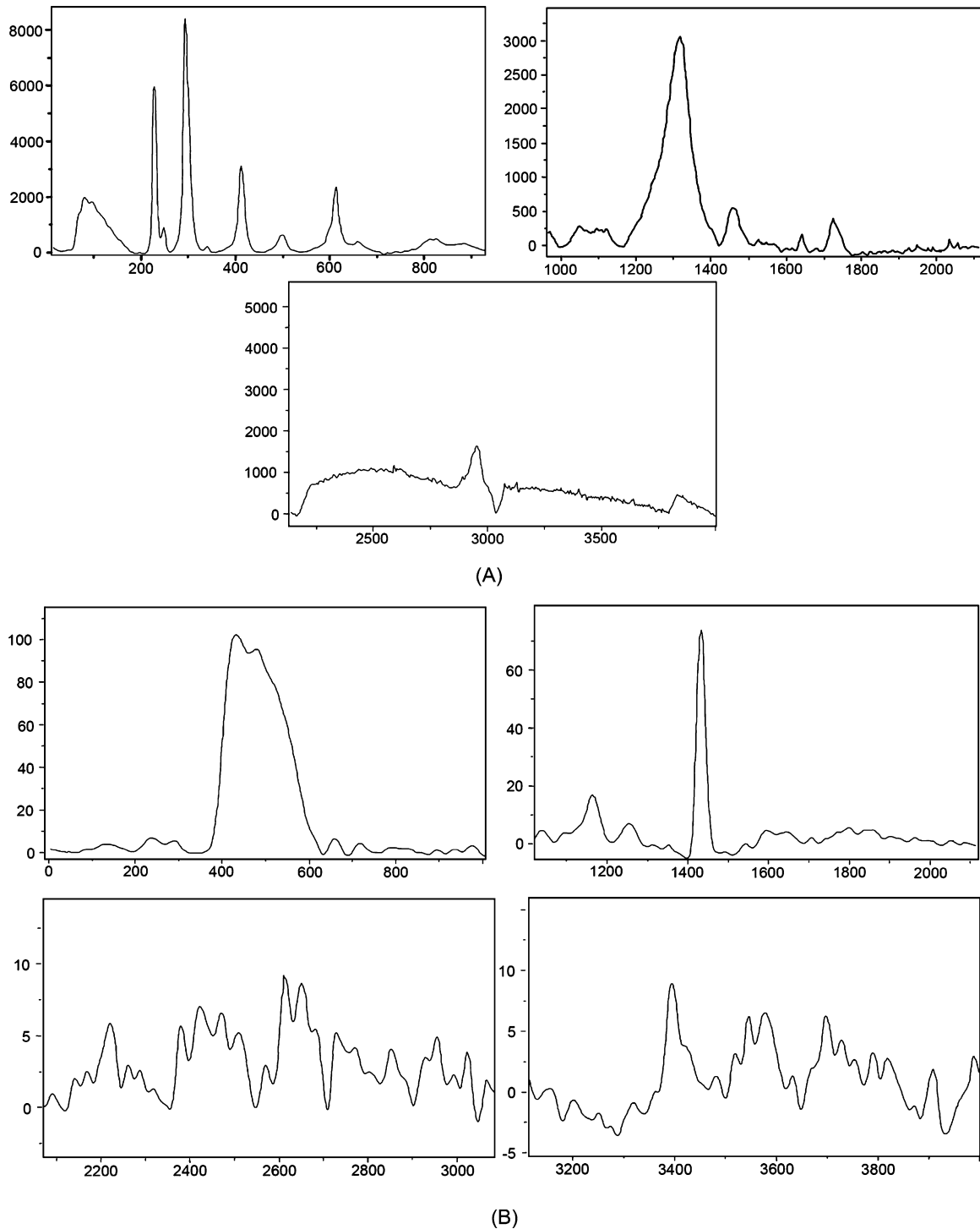


Fig. 3. Raman spectrum of: (A) mPHEMA beads; (B) Cibacron Blue F3GA-attached mPHEMA beads.

stretching vibration frequencies of the C–H groups were also seen but detailed evaluation is not performed.

3.3. Adsorption of lysozyme from aqueous solutions

3.3.1. Effect of pH

The amount of lysozyme adsorbed onto the Cibacron Blue F3GA-attached mPHEMA beads as a function of pH was shown

in Fig. 4. Lysozyme is positively charged at pH 7.0 (isoelectric point of lysozyme: 11.2). But it is interesting to note that the amount of lysozyme adsorbed onto Cibacron Blue F3GA-attached mPHEMA beads shows a maximum at pH 7.0, with a significant decrease at lower and higher pH values. Specific interactions (hydrophobic, electrostatic and hydrogen bonding) between lysozyme and dye molecules at pH 7.0 may be resulted both from the ionization states of several groups on both the

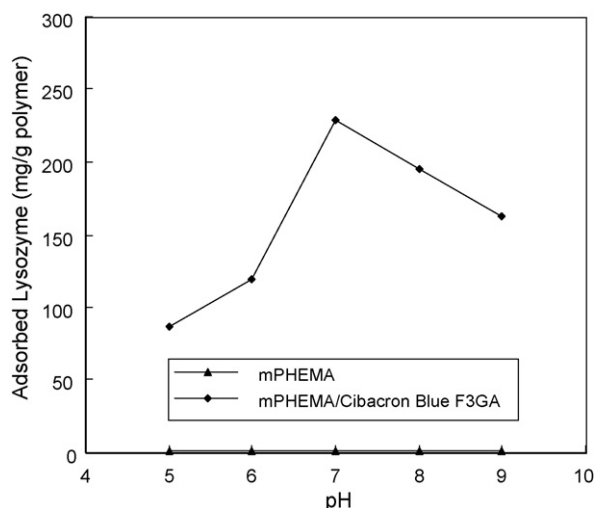


Fig. 4. Effect of pH on lysozyme adsorption. Lysozyme concentration: 1.0 mg/ml; Cibacron Blue F3GA loading: 28.5 μ mol/g; flow-rate: 1.0 ml/min; T: 25 °C.

Cibacron Blue F3GA (i.e., sulfonic acid and amino) and amino acid side chains in lysozyme, and from the conformational state of lysozyme molecules (more folded structure) at this pH. Depending on its amino acid composition, a protein can have several charged groups at the pI , the spatial arrangement of which is a function of primary, secondary, tertiary and quaternary structure. Therefore, the interaction of a protein with an affinity system may not occur at its pI value. Lysozyme molecule has one histidine, four aspartic acid, two glutamic acid and two tyrosine residues (on the basis of its surface accessible residues). These amino acid side chains of lysozyme molecules could cause other type of interactions with low percentage according to the hydrophobic interactions. At pH values lower and higher than pH 7.0, the adsorbed amount of lysozyme drastically decreases. This could be created from the ionization state of lysozyme and could be caused repulsive electrostatic forces between lysozyme and the dye molecules. Increase in conformational size and the electrostatic repulsion effects between the opposite charged groups may also cause a decrease in adsorption efficiency.

3.3.1.1. Effects of lysozyme concentration. Fig. 5 shows the lysozyme adsorption isotherm of the plain and dye-affinity beads. Note that one of the main requirements in dye-affinity chromatography is the specificity of the affinity adsorbent for the target molecule. The non-specific interaction between the support, which is the mPHEMA beads in the present case, and the molecules to be adsorbed, which are the lysozyme molecules here should be minimum in order to consider the interaction as specific. As seen in this figure, negligible amount of lysozyme was adsorbed non-specifically on the mPHEMA beads, which was 0.8 mg/g. While dye-immobilization significantly increased the lysozyme binding capacity of the mPHEMA beads (up to 342 mg/g). The amount of lysozyme adsorbed per unit mass of the mPHEMA beads increased first with the initial concentration of lysozyme then reached a plateau value which represents saturation of the active adsorption sites (which are available and accessible for lysozyme) on the magnetic beads. This increase

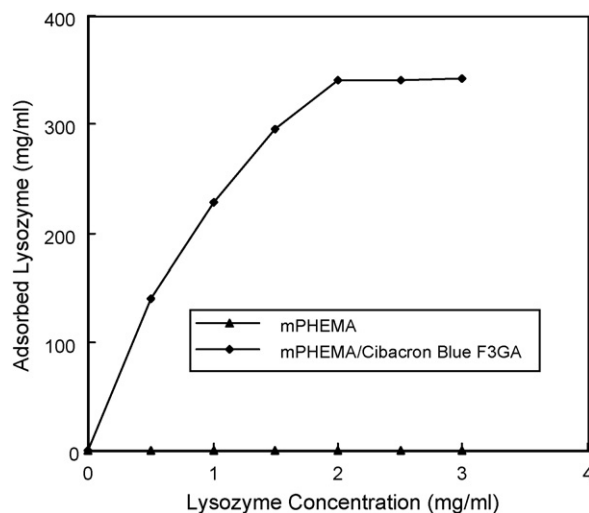


Fig. 5. Effect of the concentration of lysozyme on the lysozyme adsorption. Cibacron Blue F3GA loading: 28.5 μ mol/g; flow-rate: 1.0 ml/min; pH: 7.0; T: 25 °C.

in the lysozyme coupling capacity may have resulted from cooperative effect of different interaction mechanisms such as hydrophobic, electrostatic and hydrogen bonding caused by the acidic groups and aromatic structures on the Cibacron Blue F3GA and by groups on the side chains of amino acids on the lysozyme molecules. It should be mentioned that Cibacron Blue F3GA is not very hydrophobic overall, but it has planar aromatic surfaces that prefer to interact with hydrophobic groups in lysozyme structure.

3.3.1.2. Effect of flow-rate. The adsorption amounts of lysozyme at different flow-rates are given in Fig. 6. Results show that the lysozyme adsorption capacity onto the Cibacron Blue F3GA-attached mPHEMA beads decreases when the flow-rate through the column increases. The adsorption capacity decreased significantly from 279 mg/g to 140 mg/g polymer with the increase of the flow-rate from 0.5 ml/min to 3.5 ml/min. An

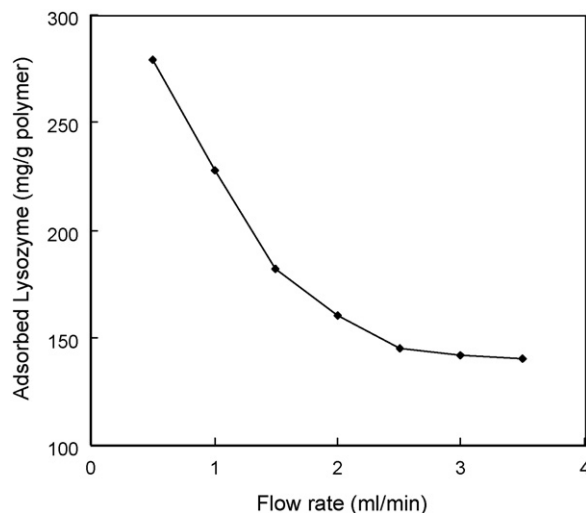


Fig. 6. Effect of flow-rate on lysozyme adsorption. Cibacron Blue F3GA loading: 28.5 μ mol/g; lysozyme concentration: 1.0 mg/ml; pH: 7.0; T: 25 °C.

increase in the flow-rate reduces the solution volume treated efficiently until breakthrough point and therefore decreases the service time of beads column. This is due to decrease in contact time between the lysozyme molecules and the Cibacron Blue F3GA-attached mPHEMA beads at higher flow-rates. These results are also in agreement with those referred to the literature [25]. When the flow-rate decreases the contact time in the column is longer. Thus, lysozyme molecules have more time to diffuse to the pore walls of beads and to bind to the binding sites of adsorbent, hence a better adsorption capacity is obtained. In addition, for column operation the magnetic bed is continuously in contact with a fresh protein solution. Consequently the concentration in the solution in contact with a given layer of beads in a column is relatively constant. For batch treatment, the concentration of solute in contact with a specific quantity of adsorbent steadily decreases as adsorption proceeds, thereby decreasing the effectiveness of the adsorbent for removing the solute.

3.3.2. Effect of NaCl concentration

The effect of NaCl concentration on lysozyme adsorption is presented in Fig. 7, which shows that the adsorption capacity decreases with increasing ionic strength of the binding phosphate buffer. The adsorption amount of lysozyme decreased by about 35.5% as the NaCl concentration changes from 0.01 M to 0.1 M. Increasing the NaCl concentration could promote the adsorption of the dye molecules to the polymer surface by hydrophobic interaction. Moreover, the hydrophobic interactions between the immobilized dye molecules themselves would also become strong, because it has been observed that the salt addition to a dye solution caused the stacking of the free dye molecules. Thus, the numbers of the immobilized dye molecules accessible to lysozyme would decrease as the ionic strength increased, and the adsorption of the lysozyme to immobilized dye became difficult. It is also suggested that an increase in NaCl concentration result in the reduction of electrostatic interactions due to Debye screening effect [26].

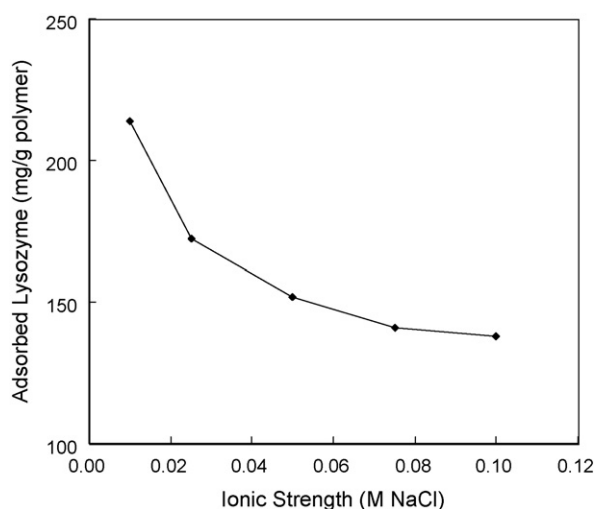


Fig. 7. Effect of the NaCl concentration on lysozyme adsorption. Cibacron Blue F3GA loading: 28.5 $\mu\text{mol/g}$; lysozyme concentration: 1.0 mg/ml; pH: 7.0; flow-rate: 1.0 ml/min; T : 25 $^{\circ}\text{C}$.

3.3.3. Desorption and reusability of adsorbents

In order to test the reusability of the beads, lysozyme adsorption–desorption procedure was repeated 20 times by using the same beads. At the end of 20 adsorption–desorption cycle, there was no remarkable reduce in the adsorption capacity. The loss of adsorption capacity during these stages was only 2.8%.

To evaluate the effects of the adsorption conditions on the lysozyme structure, fluorescence spectrophotometry was used. The fluorescence spectra of lysozyme sample obtained from the desorption step was recorded. The fluorescence spectra of native and heat-denatured lysozyme (at 72 $^{\circ}\text{C}$) were also recorded. A clear difference was observed between the fluorescence spectra of native lysozyme and heat-denatured lysozyme. An appreciable shift was seen in the maximum wavelength of denatured lysozyme with respect to the native one. However, the fluorescence spectra of the sample withdrawn from the desorption step was very close to those of native lysozyme, and no significant shift of the maximum wavelength was detected in the spectra of these samples in comparison with that of native lysozyme. It may be concluded that dye-affinity chromatography with mPHEMA beads can be applied to lysozyme separation without any conformational changes or denaturation.

3.3.4. Adsorption of lysozyme from egg white

The content of lysozyme in chicken egg white is about 3.4%. The classical lysozyme purification method required several steps, such as precipitation, centrifugation and affinity adsorption [27]. In this study, lysozyme purification from egg white was studied in a batch mode. The purity of the lysozyme eluted from dye-affinity beads was determined by SDS-PAGE (Fig. 8). The purity of the desorbed lysozyme was about 87.4% with recovery about 79.6%. The dye-affinity beads provided an efficient method to purify lysozyme from diluted egg white, showing high adsorption capacity and high selectivity for lysozyme. The specific activity of the purified lysozyme with dye-affinity was 41.586 U/mg. It should be noted that the specific activity of native lysozyme was 46.500 U/mg. As seen here there was no drastic decrease in specific activity during the purification studies.

3.3.5. Comparison of magnetically stabilized fluidized bed and batch system

Column-type continuous flow operations appear to have a distinct advantage over batch type operations because the rate of adsorption depends on the concentration of solute in solution being treated [28]. For column operation the adsorbents are continuously in contact with a fresh solution. Consequently the concentration in the solution in contact with a given layer of adsorbent in a column is relatively constant. For batch treatment, the concentration of solute in contact with a specific quantity of adsorbent steadily decreases as adsorption proceeds, thereby decreasing the effectiveness of the adsorbent for removing the solute. The MSFB column capacity (228 mg lysozyme/g polymer) was found to be higher than the batch capacity (208 mg lysozyme/g polymer). This means, in equilibrium binding experiments, maximum adsorption capacity for batch system was 9.6% lower as compared to the value obtained in MSFB.

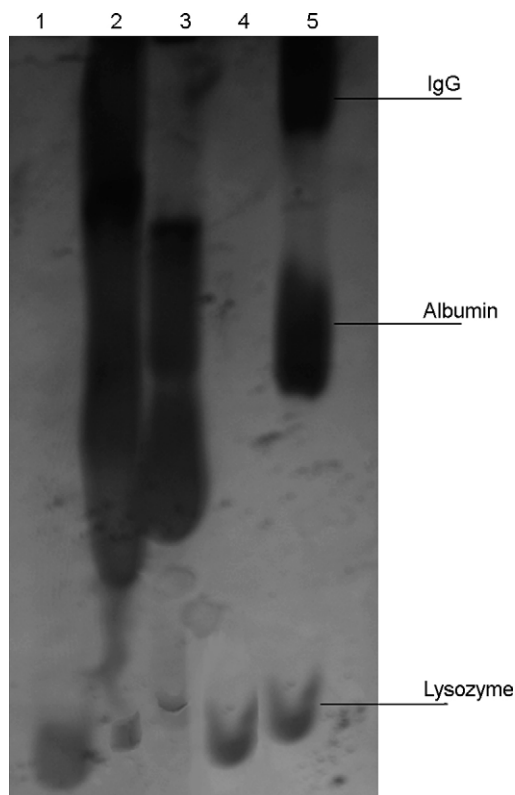


Fig. 8. SDS/PAGE of lysozyme. The purity of lysozyme was assayed by SDS/PAGE using 10% separating gel (9 cm × 7.5 cm) and 6% stacking gels were stained with 0.25% (w/v) Coomassie Brilliant R 250 in acetic acid–methanol–water (1:5:5, v/v/v) and destained in ethanol–acetic acid–water (1:4:6, v/v/v). Lane 1, commercial lysozyme; lane 2, egg white before adsorption; lane 3, egg white after adsorption; lane 4, desorbed lysozyme; lane 5 commercial marker. Equals amounts of sample were applied to each line.

The higher column capacity may be due to the fact that the continuously large concentration gradient at the interface zones occurred as to passes through the column, while the concentration gradient decreases with time in batch experiments.

4. Conclusions

A wide variety of functional molecules, including enzymes, coenzymes, cofactors, antibodies, amino acid derivatives, oligopeptides, proteins, nucleic acids, and oligonucleotides may be used as ligands in the design of novel adsorbents [8,29–31]. These ligands are extremely specific in most cases. However, they are expensive, due to high cost of production and/or extensive purification steps. In the process of the preparation of specific adsorbents, it is difficult to immobilize certain ligands on the supporting matrix with retention of their original biological activity [30]. Precautions are also required in their use (at adsorption and elution steps) and storage. Dye–ligands have been considered as one of the important alternatives to natural counterparts for specific affinity chromatography to circumvent many of their drawbacks, mentioned above [32]. Dye–ligands are able to bind most types of proteins, especially enzymes, in some cases in a remarkably specific manner. They are commercially available, inexpensive, and can easily be immobilized,

especially on matrices bearing hydroxyl groups [33]. Although dyes are all synthetic in nature, they are still classified as affinity ligands because they interact with the active sites of many proteins by mimicking the structure of the substrates, cofactors, or binding agents for those proteins [34]. The triazine dye, Cibacron Blue F3GA-attached mPHEMA beads provided an efficient method to separate lysozyme, showing high binding capacity, assuring a purity of about 87.4% with recovery about 79.6%. In order to examine the effect of adsorption/desorption conditions on conformational changes of lysozyme molecules, fluorescence spectrophotometry was employed. It appears that the dye-affinity chromatography under magnetic fields can be applied for the adsorption of lysozyme without causing any denaturation. Repeated adsorption/desorption processes showed that dye-attached mPHEMA beads are suitable for lysozyme adsorption.

References

- [1] M. Wilchek, T. Miron, *React. Func. Polym.* 41 (1999) 263.
- [2] A. Denizli, E. Pişkin, *J. Biochem. Biophys. Method* 49 (2001) 391.
- [3] L. Uzun, H. Yavuz, R. Say, A. Ersöz, A. Denizli, *Ind. Eng. Chem. Res.* 43 (2004) 6507.
- [4] S. Emir, R. Say, H. Yavuz, A. Denizli, *Biotechnol. Prog.* 20 (2004) 223.
- [5] H. Yavuz, A. Denizli, *Macromol. Biosci.* 4 (2004) 84.
- [6] S. Oncel, L. Uzun, B. Garipcan, A. Denizli, *Ind. Eng. Chem. Res.* 44 (2005) 7049.
- [7] C. Hidayat, M. Nakajima, M. Takagi, T. Yoshida, *J. Biosci. Bioeng.* 95 (2003) 133.
- [8] R.M. Birch, C. O'Byrne, I.R. Booth, P. Cash, *Proteomics* 3 (2003) 764.
- [9] F.J. Wolman, M. Graselli, O. Cascone, *Process Biochem.* 41 (2006) 356.
- [10] M. Glanzel, R. Bultmann, K. Starke, A.W. Frahm, *Eur. J. Med. Chem.* 38 (2003) 303.
- [11] R. Ghosh, Z.F. Cui, *J. Membr. Sci.* 167 (2000) 47.
- [12] R. Ghosh, S.S. Silva, C.F. Cui, *Biochem. Eng. J.* 6 (2000) 19.
- [13] S. Das, S. Banerjee, J. Dasgupta, *Chemotherapy* 38 (1992) 350.
- [14] F. Cartei, G. Cartei, V. Ceschia, S. Pacor, G. Sava, *Curr. Therap. Res. Clin. Exp.* 50 (1991) 530.
- [15] F. Murakami, T. Sasaki, T. Sugahara, *Cytotechnology* 24 (1997) 177.
- [16] B. Xue, Y. Sun, *J. Chromatogr. A* 921 (2001) 109.
- [17] P. Prikryl, D. Horak, M. Ticha, Z. Kucerova, *J. Sep. Sci.* 29 (2006) 2541.
- [18] M. Odabasi, A. Denizli, *J. Chromatogr. B* 760 (2001) 137.
- [19] S. Akgöl, A. Denizli, *J. Mol. Catal. B* 28 (2004) 7.
- [20] I. Safarik, M. Safarikova, F. Weyda, E.M. Szablewska, A.S. Waniewska, *J. Magn. Magn. Mater.* 293 (2005) 371.
- [21] X.D. Tong, B. Xue, Y. Sun, *Biotechnol. Prog.* 17 (2001) 134.
- [22] A. Denizli, *J. Chromatogr. B* 772 (2002) 357.
- [23] A. Denizli, R. Say, E. Pişkin, *React. Func. Polym.* 55 (2003) 99.
- [24] R.M. Solbrig, L.L. Duff, D.F. Shriver, I.M. Klotz, *J. Inorg. Chem.* 17 (1982) 69.
- [25] E. Valdman, L. Erijman, F.L.P. Pessoa, S.G.F. Leite, *Process Biochem.* 36 (2001) 869.
- [26] Z. Guo, Y. Sun, *Biotechnol. Prog.* 20 (2004) 500.
- [27] S. Senel, B. Elmas, T. Çamlı, M. Andaç, A. Denizli, *Sep. Sci. Technol.* 39 (2004) 3783.
- [28] M. Ahmaruzzaman, D.K. Sharma, *J. Colloids Interf. Sci.* 287 (2005) 14.
- [29] C.Y. Wu, S.Y. Suen, S.C. Chen, J.H. Tzeng, *J. Chromatogr. A* 996 (2003) 53.
- [30] H. Yavuz, A. Denizli, *Macromol. Biosci.* 5 (2005) 39.
- [31] A. Denizli, S. Senel, Y. Arica, *Colloids Surf. B* 11 (1998) 113.
- [32] M. Odabasi, A. Denizli, *J. Appl. Polym. Sci.* 93 (2004) 719.
- [33] Z.Y. Ma, Y.P. Guan, H.Z. Liu, *React. Func. Polym.* 66 (2006) 618.
- [34] A. Denizli, G. Köktürk, H. Yavuz, E. Pişkin, *J. Appl. Polym. Sci.* 74 (1999) 2803.